5824 *Inorg. Chem.* **2010**, *49*, 5824–5833
DOI: 10.1021/ic901525p

Inorganic Chemistry
Article

Photochromism, Electrical Properties, and Structural Investigations of a Series of Hydrated Methylviologen Halobismuthate Hybrids: Influence of the Anionic Oligomer Size and Iodide Doping on the Photoinduced Properties and on the Dehydration Process

Nicolas Leblanc,[†] Wenhua Bi,[†] Nicolas Mercier,*[,†] Pascale Auban-Senzier,[‡] and Claude Pasquier[‡]

[†]*Institut des Sciences et Technologies Moléculaires d'Angers, MOLTECH Anjou, UMR-CNRS 6200, Université d'Angers, 2 Bd Lavoisier, 49045 Angers, France, and* [‡]*Laboratoire de Physique des Solides, UMR-CNRS 8502, Bât. 510, Université Paris Sud, 91405 Orsay Cedex, France*

Received July 31, 2009

Syntheses, X-ray structural analyses, thermal behaviors, photochromism, and electrical properties of a series of methylviologen (MV^{2+}) halobismuthate hybrids, namely, $(MV)_3[Bi_4Cl_{18}](H_2O)_y$ (**1a**, $y \cong 1.7$), $(MV)_4[Bi_6Cl_{26}](H_2O)_y$ (**2a**, $y \cong 1.7$), $(MV)_4[Bi_6Cl_{25.6}I_{0.4}](H_2O)_y$ (**3a**, $y \cong 1.5$), and $(MV)_4[Bi_6Cl_{24.6}I_{1.4}](H_2O)_y$ (**4a**, $y \cong 1.3$), are reported. Because of the thermal effect of a UV lamp or as a result of being heated up to 100 °C, all of the above compounds undergo a complete (**1a**, **2a**, and **3a**) or a partial (**4a**) dehydration together, in **2a** and **3a**, with an impressive structural reorganization involving a 90° rotation of methylviologen dimers and, in **3a**, a new Cl/I distribution, finally leading to $(MV)_3[Bi_4Cl_{18}]$ (**1b**), $(MV)_4[Bi_6Cl_{26}]$ (**2b**), $(MV)_4[Bi_6Cl_{25.6}I_{0.4}]$ (**3b**), and $(MV)_4[Bi_6Cl_{24.6}I_{1.4}](H_2O)_x$ (**4a**, $x \cong 0.65$), respectively. In its turn, **4a** ($x \cong 0.65$) undergoes an abrupt structural change at 160 °C when water molecules are completely removed, leading to $(MV)_4[Bi_6Cl_{24.6}I_{1.4}]$ (**4b**). Obviously, the two first dehydrated phases can be considered as the $n = 2$ (**1b**) and $n = 3$ (**2b**) members of the $(MV)_{(2n+2)/2}[Bi_{2n}Cl_{8n+2}]$ family, and the ultimate member ($n = \infty$) with an infinite 1D double-chain inorganic framework, namely, $(MV)[Bi_2Cl_8]$, has already been reported. According to the results of structural refinements, some positions of the Cl atoms in the $[Bi_6Cl_{26}]^{8-}$ anionic cluster of **3a** and **4a** have been occupied by I atoms, finally leading to iodide-doped materials of the **2a** type (percentage of doping: **3a**, 1.5%; **4a**, 5.4%). Upon UV irradiation, yellow crystals of **2a** and **3a** (which become **2b** and **3b** because of the thermal effect of the UV lamp) or yellow crystals of **2b**, **3b**, and **4a** undergo a color change to black crystals (in the case of **2b**), as observed in $(MV)[Bi_2Cl_8]$, or light-brown crystals (in the cases of **3b** and **4a**). These photochromic properties are probably due to the photoinduced electron transfer from the anionic part to the methylviologen dications. In contrast, no color change is observed when yellow crystals of **1a** or **1b** and the iodide-doped $(MV)[Bi_2Cl_{8-\varepsilon}I_\varepsilon]$ material are irradiated. Because the relative positions of methylviologen to the host anionic frameworks are comparable in all structures (the N···Cl distances are about 3.4 Å), these results indicate that such kinds of photochemical reactions depend on the dimension of the anionic networks, as well as the iodide doping. The single-crystal electrical conductivity measurements of **2b** before and after irradiation were carried out between 150 and 393 K. The results prove that both of them are semiconductors with weak room temperature conductivity and that the band gap of the irradiated crystal (**2b**, 0.35 eV) is much smaller than that of the original hybrid **2a** (1.0 eV).

Introduction

Organic−inorganic hybrids are interesting systems because of the opportunity to combine the distinctive properties of both components into one material. Focusing on halometalate hybrids, those based on Sn^{II}, Pb^{II}, Sb^{III}, and Bi^{III} ions have demonstrated special attraction in the recent past as materials for optics[1,2] or electronics.[3,4] The organic entities, which are typically optically and electrically inert molecules with large band gaps, behave as weakly interacting individual

*To whom correspondence should be addressed. E-mail: nicolas.mercier@univ-angers.fr. Fax: 33.(2).41.73.54.05. Tel: 33.(2).41.73.50.83.

(1) Bi, W.; Louvain, N.; Mercier, N.; Luc, J.; Rau, I.; Kajzar, F.; Sahraoui, B. *Adv. Mater.* **2008**, *20*, 1013.

(2) (a) Cariati, E.; Ugo, R.; Cariati, F.; Roberto, D.; Masciocchi, N.; Galli, S.; Sironi, A. *Adv. Mater.* **2001**, *13*, 1665. (b) Guloy, A. M.; Tang, Z.; Mirana, B.; Srdanov, V. I. *Adv. Mater.* **2001**, *13*, 833.

(3) Kojima, A.; Teshima, K.; Shirai, Y.; Miyasaka, T. *J. Am. Chem. Soc.* **2009**, *131*, 6050.

(4) (a) Mitzi, D. B. *J. Mater. Chem.* **2004**, *15*, 2355. (b) Kagan, C. R.; Mitzi, D. B.; Chondroudis, K. *Science* **1999**, *286*, 945. (c) Mitzi, D. B.; Chondroudis, K.; Kagan, C. R. *IBM J. Res. Dev.* **2001**, *45*, n°1.

Published on Web 06/01/2010

molecules, helping the self-assembly of materials. One of the successful strategies to achieve new materials is the incorporation of functional organic entities able to enhance collective properties of the whole material as well as bring new properties resulting from the synergy of both organic and inorganic components. For instance, because of their chiral conformation, cystaminium cations bear crucial responsibility for the nonlinear optical properties of their corresponding iodometalate salts.[1,5] Some electron-donor-extended π-linear-conjugated molecules, such as thiophene[6] or tetrathiafulvalene[7] derivatives, were also introduced into these hybrid systems with the aim of enhancing their semiconducting properties. With regards to electron-acceptor organic entities, several halo(or pseudohalo-)metalate salts with charge-transfer (CT) abilities based on a methylviologen dication have been reported in pioneer works,[8] as well as in more recent works.[9−11]

The electron-acceptor methylviologen dication has afforded a great number of CT complexes that have been extensively examined in solution for a better understanding of the electron-transfer processes in CT complexes.[12] Crystalline viologen salts have also been studied, especially those based on inorganic host frameworks able to incorporate viologen guest cations, either through exchange reaction in zeolite-type compounds[13] or during the crystallization process in polycyanocadmate-type anionic host-network-based compounds.[14−16] Most of these crystals also incorporate neutral guest molecules, which often interact with the viologen dications, giving CT complex guests and possibly leading to photochromism.[16] This photochromism phenomenon was also known in a viologen-containing solution as well as in a solid-state matrix such as cellulose or silica gel.[17] It is explained by the presence of $MV^{\cdot+}$, which has a broad absorption band centered at 600 nm in the visible range, resulting from a photoinduced CT.[10,12,16−18] Photochromism can also be observed in crystallized compounds with viologen dications only surrounded by anionic host frameworks.[10,16b,18] A good example is the 1D methylviologen chlorobismuthate $(MV)[Bi_2Cl_8]$, which undergoes an impressive color change, from yellow to black upon UV irradiation.[10] In these compounds, while a quite short N (viologen)$\cdots$X (element of the host) seems to be necessary for the observation of photochromism, there are no other common structural features corresponding to this phenomenon. For instance, while a planar geometry of MV^{2+} is a favorable parameter for the observation of photochromism, because $MV^{\cdot+}$ is more stable in this geometry,[19] photoinduced reduction of MV^{2+} has been already observed in a compound incorporating MV^{2+} with a dihedral angle of 50°.[16b]

In this Article, we report the syntheses, crystal structures, thermal behaviors, photochromism, and electrical properties of a series of methylviologen (MV^{2+}) halobismuthate hybrids whose structures can be related to $(MV)[Bi_2Cl_8]$ by the dimensional reduction concept. In the first part, the structures of $(MV)_3[Bi_4Cl_{18}](H_2O)_y$ (**1a**, $y \cong 1.7$), $(MV)_4[Bi_6Cl_{26}](H_2O)_y$ (**2a**, $y \cong 1.7$), $(MV)_4[Bi_6Cl_{25.6}I_{0.4}](H_2O)_y$ (**3a**, $y \cong 1.5$), and $(MV)_4[Bi_6Cl_{24.6}I_{1.4}](H_2O)_y$ (**4a**, $y \cong 1.3$), together with their thermal behaviors, leading to the dehydrated phases $(MV)_3[Bi_4Cl_{18}]$ (**1b**), $(MV)_4[Bi_6Cl_{26}]$ (**2b**), $(MV)_4[Bi_6Cl_{25.6}I_{0.4}]$ (**3b**), and $(MV)_4[Bi_6Cl_{24.6}I_{1.4}]$ (**4b**), are described. We will show that the structures of all of these chlorobismuthate and iodide-doped chlorobismuthate salts are based on inorganic clusters consisting of *n* subunits, each formed by two edge-shared BiX_6 (X = Cl, I) octahedra, which are linked together via an octahedral corner-sharing mode, and, moreover, that all of the methylviologen dications are nearly planar. In the second part, UV irradiation effects of samples will be discussed. We will show that yellow crystals of **2a** or **2b**, **3a** or **3b**, and **4a** or **4b** were transformed into black crystals (in the case of **2a**/**2b**) or light-brown crystals (in the cases of **3a**/**3b** and **4a**/**4b**), while no photochromism is observed for **1a**/**1b** and the iodide-doped $(MV)[Bi_2Cl_{8-\varepsilon}I_\varepsilon]$ sample, thus highlighting the influence of the size of the anionic network and the iodide doping on the photochromic properties. Finally, the results of electrical conductivity measurements on a single crystal of **2b** before and after irradiation, which indicate clearly the impact of irradiation on the band gap of both materials, are reported.

Experimental Section

Synthesis and Thermal and Powder X-ray Diffraction (PXRD) Characterizations. All compounds were prepared by a solvothermal method using a Teflon-lined PARR autoclave (internal volume 25 mL). **1a** and **2a**: To 0.6 mmol of $BiCl_3$ (98%; MW = 315.33, 193.06 mg) and 0.6 mmol (**1a**) and 0.3 mmol (**2a**) of 4,4′-dipyridyl (98%, MW = 156.18, 95.62 mg and 47.81 mg) were added 10 mL of methanol and 1.68 mL of hydrochloric acid (MW = 36.16, 36 wt %, d = 1.18, 20 mmol). The autoclave was heated in a programmable oven with the following parameters: 6 h of heating from 25 to 150 °C, 13 h remaining at 150 °C, and then 10 h of cooling down to 25 °C. Yellowish crystals (**1a**) and yellow crystals (**2a**) were collected by filtration

(5) (a) Mercier, N.; Barres, A. L.; Giffard, M.; Rau, I.; Kajzar, F.; Sahraoui, B. *Angew. Chem.* **2006**, *45*, 2100. (b) Louvain, N.; Mercier, N.; Luc, J.; Sahraoui, B. *Eur. J. Inorg. Chem.* **2008**, 3592.

(6) (a) Mitzi, D. B.; Chondroudis, K.; Kagan, C. R. *Inorg. Chem.* **1999**, *38*, 6246. (b) Zhu, X. H.; Mercier, N.; Frère, P.; Blanchard, P.; Roncali, J.; Allain, M.; Pasquier, C.; Riou, A. *Inorg. Chem.* **2003**, *42*, 5330. (c) Zhu, X. H.; Mercier, N.; Allain, M.; Frère, P.; Blanchard, P.; Roncali, J.; Riou, A. *J. Solid State Chem.* **2004**, *177*, 1067.

(7) Devic, T.; Evain, M.; Moëlo, Y.; Canadell, E.; Auban-Senzier, P.; Fourmigué, M.; Batail, P. *J. Am. Chem. Soc.* **2003**, *125*, 3295.

(8) (a) Prout, C. K.; Wright, J. D. *Angew. Chem., Int. Ed. Engl.* **1968**, *7*, 659. (b) Prout, C. K.; Murray-Rust, P. *J. Chem. Soc. A* **1969**, 1520. (c) Macfarlane, A. J.; Williams, J. P. *J. Chem. Soc. A* **1969**, 1517.

(9) (a) Tang, Z.; Litvinchuk, A. P.; Lee, H.-G.; Guloy, A. M. *Inorg. Chem.* **1998**, *37*, 4752. (b) Place, H.; Scott, B.; Willet, R. D. *Inorg. Chim. Acta* **2001**, *319*, 43. (c) Scott, B.; Willet, R. D.; Saccani, A.; Sandrolini, F.; Ramakrishna, B. L. *Inorg. Chim. Acta* **1996**, *248*, 73. (d) Fujisawa, J.; Ishihara, T. *Phys. Rev. B* **2004**, *70*, 113203.

(10) (a) Xu, G.; Guo, G.; Wang, M.; Zhang, Z.; Chen, W.; Huang, J. *Angew. Chem., Int. Ed.* **2007**, *46*, 3249. (b) Wang, M.-S.; Xu, G.; Zhang, Z.-J.; Guo, G.-C. *Chem. Commun.* **2010**, *46*, 361.

(11) (a) Ju, Z.-F.; Yao, Q.-X.; Zhang, J. *Dalton Trans.* **2008**, 355. (b) Inoue, M. B.; Inoue, M.; Machi, L.; Brown, F.; Fernando, Q. *Inorg. Chim. Acta* **1995**, *230*, 145.

(12) Monk, P. M. S. *The Viologens: Physicochemical Properties, Synthesis, ans Application oft he Salt of 4,4′-Bipyridine*; Wiley: New York, 1998.

(13) (a) Park, Y. S.; Um, S. Y.; Yoon, K. B. *J. Am. Chem. Soc.* **1999**, *121*, 3193. (b) Clennan, E. L. *Coord. Chem. Rev.* **2004**, *248*, 477. (c) Alvaro, M.; Garcia, H.; Garcia, S.; Marquez, F.; Scaiano, J. C. *J. Phys. Chem. B* **1997**, *101*, 3043.

(14) Yoshikawa, H.; Nishikiori, S.; Ishida, T. *J. Phys. Chem. B* **2003**, *107*, 9261.

(15) (a) Yoshikawa, H.; Nishikiori, S. *Dalton Trans.* **2005**, 3056. (b) Yoshikawa, H.; Nishikiori, S.; Suwinska, K.; Luboradzki, T.; Lipkowski, J. *Chem. Commun.* **2001**, 1398.

(16) (a) Yoshikawa, H.; Nishikiori, S. *Chem. Lett.* **2000**, 142. (b) Yoshikawa, H.; Nishikiori, S.; Watanabe, T.; Ishida, T.; Watanabe, G.; Murakami, M.; Suwinska, K.; Luboradzki, T.; Lipkowski, J. *J. Chem. Soc., Dalton Trans.* **2002**, 1907.

(17) Yoon, K. B. *Chem. Rev.* **1993**, *93*, 321.

(18) Vermeulen, L. A.; Snover, J. L.; Sapochak, L. S.; Thomson, M. E. *J. Am. Chem. Soc.* **1993**, *115*, 11767.

(19) Ishida, T.; Murakami, M.; Watanabe, G.; Yoshikawa, H.; Nishikiori, S. *Internet Electron. J. Mol. Des.* **2003**, *2*, 14.

Table 1. Crystallographic Data for **1a**, **1b**, **2a**, **2b**, **3a**, **3b**, **4a**, and **4b**

	1a	**1b**	**2a**	**2b**
fw, g/mol	2060.03	2032.83	2952.67	2920.67
space group	$P\bar{1}$	$P\bar{1}$	$P\bar{1}$	$P\bar{1}$
a, Å	9.2783(4)	9.2588(7)	9.3993(5)	9.3871(8)
b, Å	12.5784(11)	12.5306(9)	12.613(1)	12.506(1)
c, Å	14.6518(11)	14.5781(4)	19.850(2)	19.070(3)
α, deg	72.478(8)	72.336(5)	99.77(1)	103.07(1)
β, deg	89.874(7)	89.811(6)	103.20(1)	96.16(1)
γ, deg	71.994(5)	71.266(6)	108.09(1)	108.00(1)
V, Å^3	1528.1(6)	1517.87(16)	2103.0(3)	20.35.7(4)
Z	1	1	1	1
obsd reflns [$I > 2\sigma(I)$] [R_{int}]	5786 [0.057]	5783 [0.077]	7418 [0.057]	7555 [0.070]
no. of param	310	292	420	401
R1[$I > 2\sigma(I)$]/wR2 (all data)	0.034/0.055	0.036/0.126	0.039/0.071	0.038/0.089
	3a	**3b**	**4a** ($y \cong 1.3$)	**4b**
fw, g/mol	2981.25	2957.25	3069.50	3039.56
space group	$P\bar{1}$	$P\bar{1}$	$P\bar{1}$	$P\bar{1}$
a, Å	9.3866(11)	9.3912(9)	9.4162(8)	9.4244(10)
b, Å	12.6026(8)	12.5094(9)	12.6502(9)	12.5997(10)
c, Å	19.868(2)	19.094(2)	19.955(2)	19.156(3)
α, deg	99.518(8)	103.027(7)	107.724(7)	102.979(10)
β, deg	103.518(10)	96.320(9)	103.171(8)	96.181(12)
γ, deg	108.027(7)	108.018(8)	72.189(6)	108.223(6)
V, Å^3	2100.0(4)	2038.7(4)	2131.7(3)	2066.2(4)
Z	1	1	1	1
obsd reflns [$I > 2\sigma(I)$] [R_{int}]	6134 [0.080]	5817 [0.096]	7156 [0.055]	6893 [0.074]
no. of param	452	412	452	434
R1 [$I > 2\sigma(I)$]/wR2 (all data)	0.045/0.072	0.057/0.104	0.039/0.100	0.049/0.104

and washed with methanol [yield 98% (**1a**) and 75% (**2a**) on the basis of $BiCl_3$]. Heating of **1a** and **2a** at 100 °C led to **1b** and **2b**, respectively. Anal. [scanning electron microscopy/energy-dispersive X-ray (SEM/EDX) method]. Calcd for **1b**: Bi, 40.81; Cl, 31.16. Found: Bi, 40.19; Cl, 30.22. Calcd for **2b**: Bi, 42.93; Cl, 31.56. Found: Bi, 42.27; Cl, 30.66. **3a**: To 0.6 mmol of $BiCl_3$ (98%; MW = 315.33, 193.06 mg) and 0.4 mmol of 4,4′-dipyridyl (98%, MW = 156.18, 463.75 mg) were added 10 mL of methanol, 1.68 mL of hydrochloric acid (MW = 36.16, 36 wt %, d = 1.18, 20 mmol), and 0.07 mL of hydroiodic acid (MW = 127.91, 57 wt %, d = 1.70, 0.53 mmol). Parameters of synthesis: 6 h of heating from 25 to 150 °C, 19 h remaining at 150 °C, and then 10 h of cooling down to 25 °C. Yellow crystals were collected by filtration and washed with methanol (yield 85% on the basis of $BiCl_3$). **3b** was obtained by heating **3a** at 100 °C. Anal. (SEM/EDX method). Calcd for **3b**: Bi, 42.40; Cl, 30.69; I, 1.72. Found: Bi, 40.07; Cl, 30.50; I, 1.63. **4a**: To 0.6 mmol of $BiCl_3$ (98%; MW = 315.33, 193.06 mg) and 0.4 mmol of 4,4′-dipyridyl (98%, MW = 156.18, 63.75 mg) were added 10 mL of methanol, 1.68 mL of hydrochloric acid (MW = 36.16, 36 wt %, d = 1.18, 20 mmol), and 0.14 mL of hydroiodic acid (MW = 127.91, 57 wt %, d = 1.70, 1.1 mmol). Parameters of synthesis: 2 h of heating from 25 to 150 °C, 13 h remaining at 150 °C, and then 10 h of cooling down to 25 °C. Yellow crystals were collected by filtration and washed with methanol (yield 87% on the basis of $BiCl_3$). **4b** was obtained by heating **4a** at 160 °C: Anal. (SEM/EDX method). Calcd for**4b**: Bi, 41.13; Cl, 28.61; I, 5.83. Found: Bi, 40.06; Cl, 26.07; I, 6.51.

PXRD patterns of the samples showed that all of the observed reflections can be indexed in the unit cell parameters obtained from single-crystal X-ray diffraction (XRD) experiments (see the Supporting Information, SI). Nevertheless, let us note that the PXRD patterns of **3a** and **4a** are very close to each other and to that of **2a**, as a result of close unit cell parameters. However, the homogeneity of the samples can be testified by several facts. First, the absence of black crystals in irradiated samples of **3a** and **4a** clearly shows that the samples did not contain pure chloride crystals of **2a** (under UV irradiation, yellow crystals of **2a** are transformed into black crystals of **2b**, while yellow crystals of **3a** or **4a** are transformed into light-brown crystals). Second, the PXRD of samples **3a** and **4a** heated at 100 °C clearly show, first, that all crystallites of **3a** were transformed into the new structure of **3b** (the PXRD patterns of **3a** and **3b** are very different; see the SI), as deduced from the single crystal study, and second, that **4a** was only partially dehydrated, as expected from the single crystal study (see SI). Finally, the SEM/EDX chemical analysis method showed that crystals belonging to the same sample, either **3a** or **4a**, roughly contained the same iodide rate, in good accordance with the iodide rates found from single-crystal XRD experiments.

The photoreactions were carried out by irradiating each of the samples with a 150 W Hg lamp (TQ150 from Heraeus; strongest line at 366 nm), typically for 1 night.

Differential scanning calorimetry (DSC) and thermogravimetric analysis (TGA) were performed on DSC-2010 and TGA-2050 TA Instruments systems in the ranges of 20−300 and 20−1000 °C, respectively (see the SI). The TGA curves of **1a**, **2a**, **3a**, and **4a** are alike, with a first weight loss in the 20−150 °C range, followed by decomposition starting at about 270 °C. The first thermal accident is attributed to dehydration, with the weight loss (**1a**, 0.3354 mg; **2a**, 0.1933 mg; **3a**, 0.1384 mg; **4a**, 0.0785 mg) corresponding to 1.7 H_2O (**1a**), 1.7 H_2O (**2a**), 1.5 H_2O (**3a**), and 1.3 H_2O (**4a**) per formulation unit, respectively. It must be noted that the dehydration/rehydration process is reversible if no structural change is involved in the water dehydration. This is the case for **1a** to **1b** or for **4a** ($y \cong 1.3$) to **4a** ($y \cong 0.65$).

X-ray Crystallography. PXRD measurements were carried out on a D8 Bruker diffractometer using Cu $K\alpha_{1,2}$ radiation, equipped with a linear Vantec superspeed detector. XRD data of selected single crystals were collected on a Bruker-Nonius KAPPA-CDD diffractometer equipped with graphite-monochromated Mo Kα radiation (λ = 0.710 73 Å) at T = 293 K. A summary of crystallographic data and refinement results for all compounds is listed in Table 1. Structures were solved and refined using the *SHELXL97* package. Positions and atomic displacement parameters were refined by full-matrix least-squares routines against F^2. All hydrogen atoms were treated with a riding model in all structures. Hydrogen atoms of water molecules were not located. The oxygen atoms were first located in the general position, with a 0.5 occupation factor (higher sof

Table 2. Schematic Representation of the Dehydration Processes of **1a**, **2a**, **3a**, and **4a**

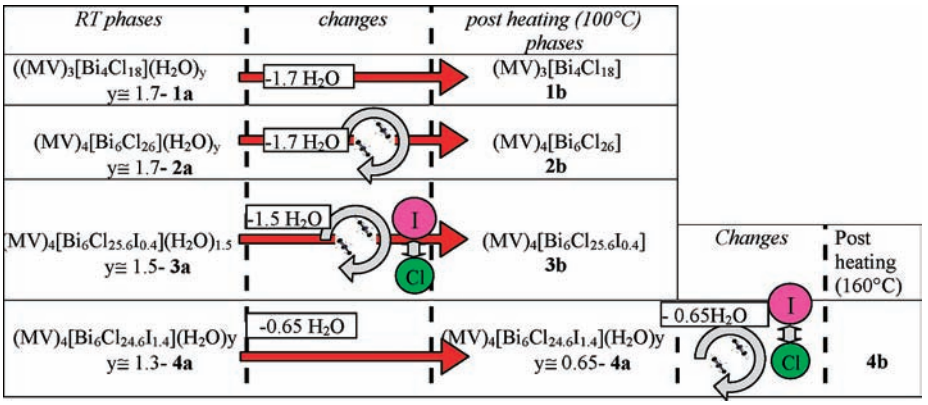

values would lead to a discrepant O−O distance in the structures), leading to equivalent isotropic agitation higher than 0.20 Å^2. Then, the sof of the oxygen atoms were refined, leading to 1.5 and 1.3 H_2O molecules per unit for **3a** and **4a**, respectively, as was found from TGA measurements, while it leads to 2 H_2O molecules per unit for **1a** and **2a**, which was greater than that obtained from TGA measurements (1.7). Finally, the sof of the oxygen atoms were fixed in all structures to match the TGA results, and we notice that the U_{eq} agitation factor for every water molecule is very close to the others and acceptable for free water molecules: U_{eq} [Å^2]/sof for the oxygen atoms in **1a**, O1 (0.151/0.43) and O2 (0.186/0.43), in **2a**, O1 (0.129/0.43) and O2 (0.154/0.43), in **3a**, O1 (0.112/0.38) and O2 (0.159/0.38), in **4a** ($y \cong 1.3$), O1 (0.130/0.33) and O2 (0.190/0.33), and in **4a** ($y \cong 0.65$), O1 (0.128/0.33)]. In iodide-containing phases, a statistical disorder affects several halide positions. For such disordered positions, the two close peaks were assigned to one chloride for the nearest peak to bismuth and to one iodide for the other. First, keeping the same isotropic agitation factor, the sof of disordered atoms was refined, with their sum being fixed to 1. Finally, refinements of the positions of all non-hydrogen atoms and of the anisotropic displacement parameters lead to R = 0.034, 0.036, 0.039, 0.038, 0.045, 0.057, 0.039, and 0.049 for **1a**, **1b**, **2a**, **2b**, **3a**, **3b**, **4a** ($y \cong 1.3$), and **4b**, respectively, and percentages of iodide doping of 1.5% and 5.4% in **3a** ($[Bi_6Cl_{25.6}I_{0.4}]^{8-}$) and **4a** ($[Bi_6Cl_{24.6}I_{1.4}]^{8-}$), respectively (note that refinements of the sof of iodine lead to 1.4 I molecules per unit in **4a** ($y \cong 1.3$) and **4a** ($y \cong 0.65$), while 1.32 I molecules were located in **4b**, indicating that a weak percentage of missing I molecules is located on other chloride positions). A summary of the room temperature crystal data of the partially dehydrated **4a** phase [$(MV)_4[Bi_6Cl_{24.6}I_{1.4}](H_2O)_x$ ($x \cong 0.65$)], obtained by heating **4a** at 100 °C, is also given in the SI. A complete list of crystallographic data, along with the atomic coordinates, anisotropic displacement parameters, and bond distances and angles for each compound, is given as CIF files.

Electrical Properties. The single-crystal conductivity of **2b**, before and after UV irradiation, was measured by applying 300 V between two contacts deposited on the surface of the crystals with a Keithley K487. The current through the samples was measured with the same apparatus in a two-point configuration. The conductivity was then extracted by considering that the current flows in the full thickness of the sample as a basic hypothesis.

Results and Discussion

Synthesis, Crystal Structures, and the Dehydration Process. Crystals of **1a**, **2a**, **3a**, and **4a** were synthesized under solvothermal conditions from $Bi^{III}Cl_3$, 4,4′-bipyridine, and concentrated HCl (**1a** and **2a**) or a mixture of concentrated HCl and HI (**3a** and **4a**) in methanol. The in situ formation of MV^{2+} dications, which has already been described as a result of the reaction of 4,4′-bipyridine, methanol, and HCl,[20] offers great advantages compared to using a methylviologen salt as the starting material, in particular for growing suitable single crystals for diffraction or conductivity measurements. The synthesis of $(MV)_3[Bi_4Cl_{18}](H_2O)_y$ ($y \cong 1.7$, **1a**) and $(MV)_4[Bi_6Cl_{26-x}I_x](H_2O)_y$ (**2a**, **3a**, and **4a**), which differentiate themselves from the Bi/MV ratio (1.33 and 1.5, respectively), could be achieved by tuning the ratio of the 4,4′-bipyridine and $BiCl_3$ starting materials (see Experimental Section). Because of the thermal effect of UV light or by heating at about 100 °C, **1a**, **2a**, **3a**, and **4a** phases undergo a complete or partial dehydration, leading to $(MV)_3[Bi_4Cl_{18}]$ (**1b**), $(MV)_4[Bi_6Cl_{26}]$ (**2b**), $(MV)_4[Bi_6Cl_{25.6}I_{0.4}]$ (**3b**), and $(MV)_4[Bi_6Cl_{24.6}I_{1.4}](H_2O)_x$ (**4a**, $x \cong 0.65$), respectively, while a temperature as high as 160 °C is necessary to completely remove water molecules in **4a** to afford $(MV)_4[Bi_6Cl_{24.6}I_{1.4}]$ (**4b**). Before the structural features of these hydrated and dehydrated phases are described in detail, it is worth noting that dramatic structural changes can be correlated with the dehydration process, which are either a rotation of viologen dimers together with a shift of inorganic blocks or a new Cl/I distribution in inorganic oligomers, and these features are summarized in Table 2.

The structures of **1b** and **2b** and the structure of $(MV)[Bi_2Cl_8]$ embody a very good example of structures related to each other by the dimensional reduction concept. This theory is a general formalism to describe the way that the M−X metal−anion framework of a parent compound is dismantled upon reaction with an AX ionic reagent to form a child compound.[21] Herein, the parent compound is $(MV)[Bi_2Cl_8]$, whose structure consists of infinite inorganic anionic chains that sandwich planar methylviologen dications (Figure 1). The inorganic network can be described as n subunits ($n = \infty$), each formed by two edge-shared $BiCl_6$ octahedra, which are linked together via an octahedral corner-sharing mode. The child compounds, $(MV)_3[Bi_4Cl_{18}]$ (**1b**) and $(MV)_4[Bi_6Cl_{26}]$ (**2b**), result from the combination of two $(MV)[Bi_2Cl_8]$ subunits and one $(MV)Cl_2$ and of three $(MV)[Bi_2Cl_8]$ subunits and one $(MV)Cl_2$, respectively. From Figures 2 and 3, we can easily appreciate that the inorganic networks in **1b** and **2b** are segments of the one-dimensional (1D)

(20) Hou, J.-J.; Guo, C.-H.; Zhang, X.-M. *Inorg. Chim. Acta* **1996**, *359*, 39.

(21) (a) Tulsky, E.; Long, J. *Chem. Mater.* **2001**, *13*, 1149. (b) Mercier, N.; Louvain, N.; Bi, W. *CrystEngComm* **2009**, *11*, 720.

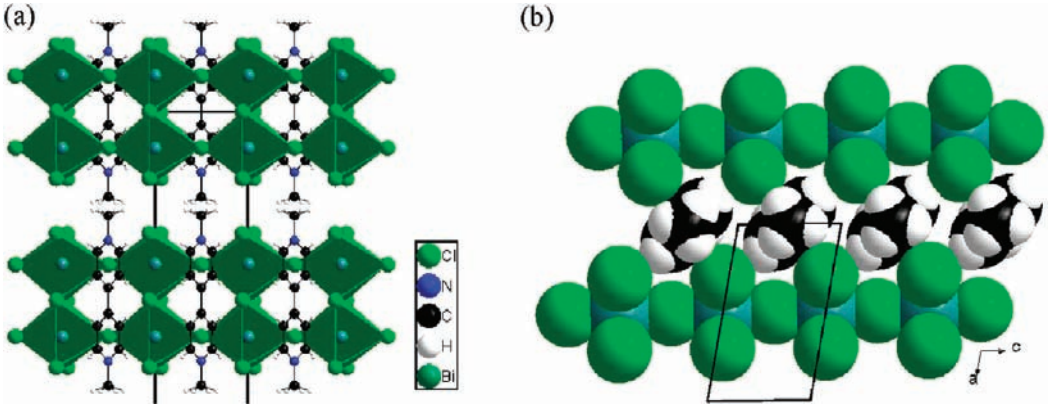

Figure 1. Structure of (MV)[Bi_2Cl_8]: general view (a) and part of the structure in a space-filling representation, showing planar methylviologen trapped between 1D chlorobismuthate chains (b).

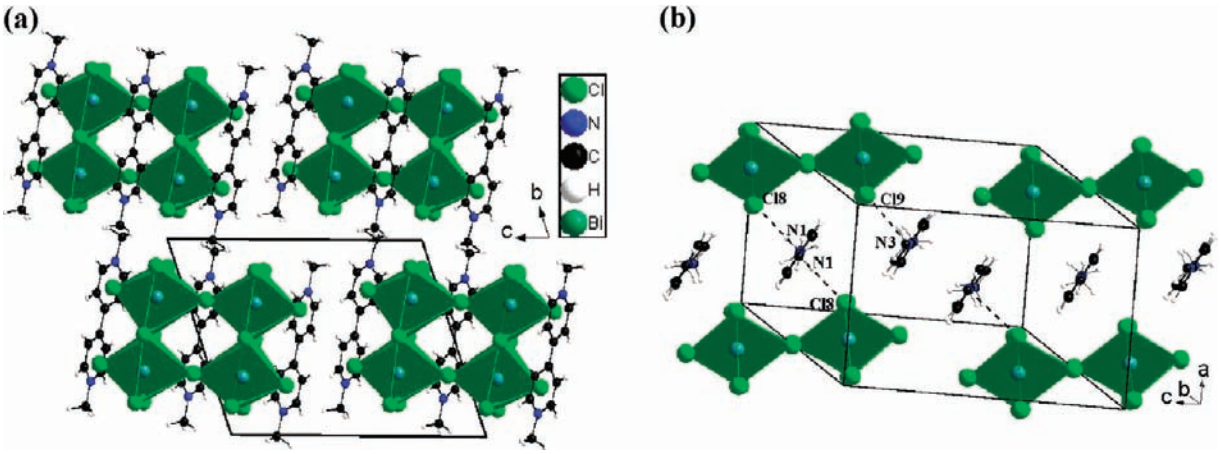

Figure 2. Structure of $(MV)_3[Bi_4Cl_{18}]$ (**1b**): general view along the *a* axis (a) and part of the structure showing the relative disposition of planar methylviologen and $[Bi_4Cl_{18}]^{6-}$ clusters in one sheet (b).

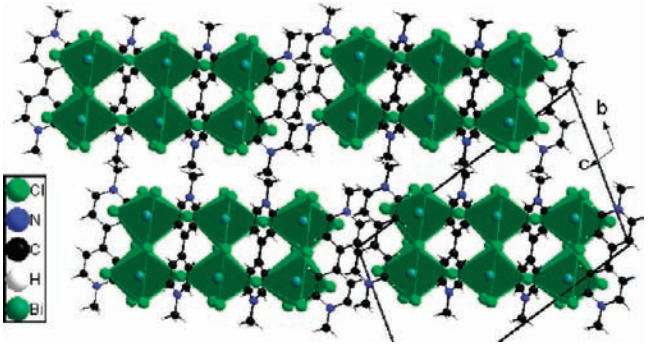

Figure 3. General view along the *a* axis of the structure of $(MV)_4[Bi_6Cl_{26}]$ (**2b**).

double chain of the parent compound (Figure 1), in such a way that, at every two subunits (**1b**) or every three subunits (**2b**), one methylviologen dichloride unit is inserted. As a consequence, the inorganic frameworks in **1b** and **2b** are oligomers of two and three subunits with the formulations of $[Bi_4Cl_{18}]^{6-}$ and $[Bi_6Cl_{26}]^{8-}$, respectively. Obviously, the two child compounds can be considered as the $n = 2$ (**1b**) and 3 (**2b**) members of the $(MV)_{(2n+2)/2}[Bi_{2n}Cl_{8n+2}]$ family, while the (MV)[Bi_2Cl_8] parent compound is the ultimate one ($n = \infty$). The overall structures of **1b** and **2b** are similar to their parent structure, and it is worth noting that the lengths of the *a* axis in all of the three structures are almost the same. Thus, the structures of **1b** and **2b** can be described as weakly interacting sheets, each consisting of methylviologen dications trapped between consecutive inorganic frameworks along the *a* axis.

Interestingly, compounds **1b** and **2b** result from dehydration of **1a** and **2a**, instead of being prepared directly. $(MV)_3[Bi_4Cl_{18}](H_2O)_y$ (**1a**,$y \cong 1.7$) losses its water molecules, which are located in the space defined by four adjacent oligomers (Figure S1 in the SI) and results in **1b**. Also, it must be noted that the dehydration process does not involve any other structural change. In contrast, the dehydration of $(MV)_4[Bi_6Cl_{26}](H_2O)_y$ (**2a**, $y \cong 1.7$) is accompanied by a dramatic structural reorganization. Similar to that in **1a**, water molecules in **2a** are located in the free space defined by four adjacent inorganic clusters of the structure viewed along the *a* axis (Figure S3 in the SI). Figure 4 shows parts of **2a** and **2b**, which is one sheet of strongly interacting organic and inorganic entities, as defined previously, viewed along the long molecular axis of viologen dications. In the hydrated phase **2a**, all molecular planes of viologen are parallel to each other, and consecutive $[Bi_6Cl_{26}]^{8-}$ clusters are shifted so that no short Cl···Cl contact involving terminal chloride is observed [d(Cl1···Cl10) = 4.382(3) Å]. After dehydration, methylviologen dimers in the interblock space (see Figure 4a) undergo an impressive 90° rotation, while at the same time, blocks shift to each other along the cleavage planes, forming a bridge between them through

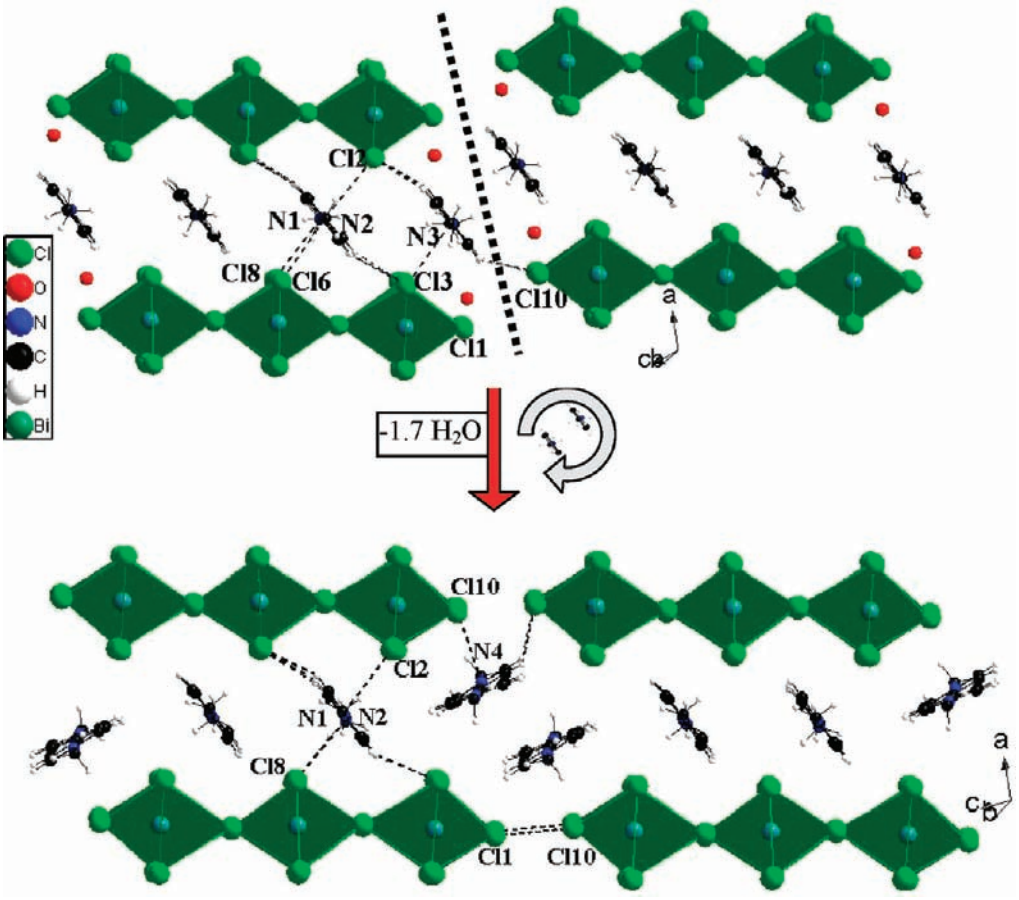

Figure 4. Parts of the structure of **2a** (top) and **2b** (down) showing the structural changes upon dehydration, in particular the 90° rotation of methylviologen dimers located in the space of the cleavage plane (dotted line).

van der Waals Cl···Cl contacts [d(Cl···Cl) = 3.574(3) Å and r_{vdw}(Cl) = 1.80 Å; Figure 4b]. Note that these two structural features are correlated to each other because the new positions of methylviologen allow $N^+ \cdots Cl_{terminal}$ interactions [d(N4···Cl10) = 3.366(3) Å], decreasing the electron charge density of the corresponding chlorides at the same time.

The structures of **3a** and **4a** differ from the one of **2a** only by the substitution of some chlorides by iodides. In $(MV)_4[Bi_6Cl_{25.6}I_{0.4}](H_2O)_y$ (**3a**, $y \cong 1.5$), three halide-independent positions (two "terminal" and one "side") of clusters are statistically occupied by both iodides and chlorides. While the dehydration process of **3a** involves a rotation of methylviologen dimers together with a shift of blocks, as in **2a**, a third structural feature occurs, which is a concerted iodide/chloride substitution in the solid state. The migration of iodides toward side halide positions of clusters (Figure 5), is probably governed by the shift of blocks, which leads to (terminal) halide−halide contacts of 3.593(3) Å (Figure S6 in the SI), and so is assigned to Cl···Cl contacts. We can also note that bulky iodide atoms located on the side position fill, in a way, the free space left by water molecules. In $(MV)_4[Bi_6Cl_{24.6}I_{1.4}](H_2O)_y$ (**4a**, $y \cong 1.3$), the number of iodides is greater than that in **3a**, and they are also located on both the terminal and side positions of clusters (Figure S8 in the SI). The consequence of this more iodide-rich compound is a complete dehydration process at higher temperature. In fact, a temperature of 100 °C, even high enough to remove approximately half the the trapped water molecule, leading to $(MV)_4[Bi_6Cl_{24.6}I_{1.4}](H_2O)_y$ (**4a**, $y \cong 0.65$), is not sufficient for activation of the complete structural reorganization, water loss, dimer rotation, block shift, and Cl/I substitution. Finally, these structural changes occur at a much higher temperature (160 °C) to give the dehydrated phase of **4b**, and as in **3b**, iodide atoms initially located on the terminal positions have moved to the side positions of clusters (Figures S8 and S9 in the SI).

Photochromism and Electrical Properties. Photochromism. Methylviologen dication (MV^{2+}), which is known as a strong electron acceptor, has afforded a great number of CT complexes.[12] MV^{2+} can be reduced by chemical or photochemical treatment into a radical cation (MV^+) with blue color. This color change, or photochromism, can be observed in solution or in a solid-state matrix such as cellulose or silica gel, as well as in crystalline samples, which are mainly hybrids based on inorganic host frameworks able to incorporate viologen guest cations, either through an exchange reaction in zeolite-type compounds[13] or during the crystallization process in polycyanocadmate-type compounds.[14−16] In the main cases, such hybrids also incorporate neutral guest molecules that form with the viologen dications so-called CT complex guests. All of these crystallized materials act as model compounds to understand CT or photoinduced CT processes at the molecular level. In particular, relationships have been established between efficient CT and weak interactions between viologen and either the host [N^+(viologen)···X (element of the host) through

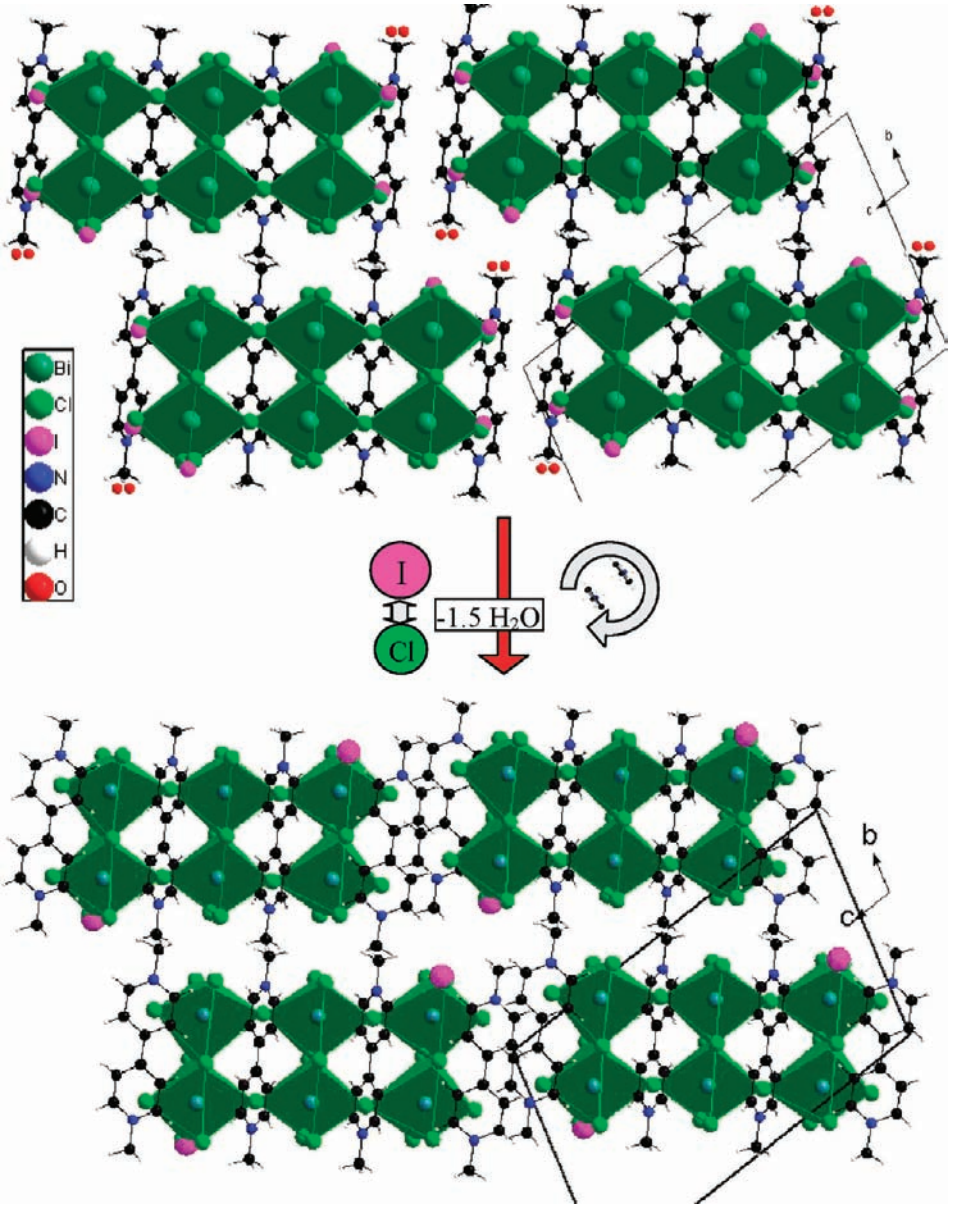

Figure 5. From $(MV)_4[Bi_6Cl_{25.6}I_{0.4}](H_2O)_y$ (**3a**, $y \cong 1.5$) to the dehydrated phase **3b**: general views of the structures showing the migration of iodides from the terminal halide positions of clusters toward the side halide positions.

$\sigma-\pi$ interaction][8a] or neutral molecules through $\pi-\pi$ interactions.[5a] Strong $\sigma-\pi$ or $\pi-\pi$ interactions in the crystal structure seem to be a necessary factor, instead of a sufficient one, to observe the photochromism phenomenon. However, several trends have been concluded. For instance, polycyanopolycadmate-type clathrates incorporating MV^{2+} and arene guests with relatively high ionization potentials were changed from colorless to blue by UV irradiation (first group), whereas those incorporating arene guests with ionization potentials lower than those of the first group, which have their own color, do not undergo a color change upon UV irradiation (second group).[15b,16]

Table 3 summarizes the photochromic properties upon UV irradiation of chlorobismuthate compounds $(MV)_{(2n+2)/2}[Bi_{2n}Cl_{8n+2}]$ (first row) and their corresponding iodide-doped compounds (second row). It is worth noting again that complete dehydration (**1a**, **2a**, and **3a** giving **1b**, **2b**, and **3b**) or partial dehydration (**4a**) occurs because of the thermal effect of UV irradiation. However, we noticed that the photochromic properties of the $n = 2$ and 3 and iodide-doped $n = 3$ compounds under UV irradiation are similar whatever the starting yellow crystals, either those of **1a**, **2a**, **3a**, and **4a** or those of **1b**, **2b**, **3b**, and **4b** (previously heated samples of **1a**, **2a**, **3a**, and **4a**). The $n = \infty$ phase, namely, $(MV)[Bi_2Cl_8]$, has been prepared according to the literature,[10a] while the corresponding doped phase was obtained by carrying out the same experiment with a trace of HI. As described in ref 10a, yellow crystals of $(MV)[Bi_2Cl_8]$ were transformed into black crystals upon UV irradiation; however, no color change for the crystals prepared in an iodide-containing solution was observed. No significant proof of an iodine atom in the structure could be found from the single-crystal XRD experiment, while the PXRD pattern of the sample was found to well fit with the calculated PXRD

Table 3. Schematic Representation of the Photochromic Properties of Chlorobismuthate Compounds $(MV)_{(2n+2)/2}[Bi_{2n}Cl_{8n+2}]$ and Related Iodide-Doped Compounds upon UV Irradiation

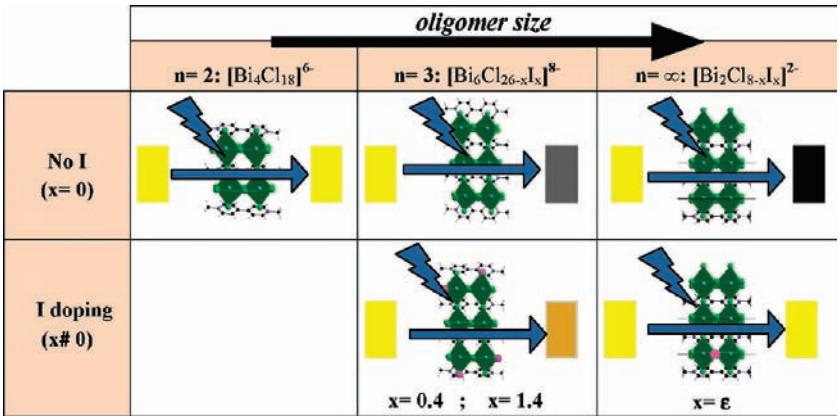

pattern of $(MV)[Bi_2Cl_8]$ (see the SI). Nevertheless, the disappearance of photochromism for these crystals very probably shows that iodide doping has occurred, with this being the cause of cancellation of the photoinduced CT process. In the case of the $n = 3$ type compounds, the iodide doping, which is of 1.5% and 5.4% for **3a**/**3b** and **4a**/**4b**, respectively, has two main effects: The first one is a color change of the samples [**3a**/**3b** and **4a**/**4b**: yellow/green instead of pale yellow (**2a**/**2b**)], as illustrated by the red shift of the main band in the UV−vis spectra of **4a** (Figure 6b, foot of the band at about 525 nm) or **3a** (see the SI), compared to the main band in the UV−vis spectrum of **2b** (Figure 6a, foot of the band at about 450 nm). The other one is a tuning of the photochromic properties because the color of the undoped $n = 3$ salt (**2a**/**2b**) turned to black while those of the iodide-doped $n = 3$ salts (**3a**/**3b** and **4a**/**4b**) turned to light brown. In both cases, the photoinduced process does not occur in the whole crystal, as shown by the color of powders resulting from the grinding of irradiated crystals: pale gray (**2b**) or yellow-green (**3b** and **4a**/**4b**). However, further irradiation of the powder samples finally gave black (**2b**) and brown powders (**3b** and **4a**/**4b**). The corresponding UV−vis spectra of irradiated **2b** and **4a** samples appear in Figure 6. In the spectrum of irradiated **2b**, a broad band around 600 nm has grown. We also note the decrease of the band at 350 nm, while a band at 310 nm appears. The peak at 600 nm is typically the signature of $MV^{\cdot+}$ corresponding to the intramolecular singly occupied molecular orbital (SOMO) to lowest unoccupied molecular orbital (LUMO) transition,[12] while the peak at 310 nm could be assigned to the highest occupied molecular orbital (HOMO) to SOMO transition of $MV^{\cdot+}$.[12] As described in previous work reporting on viologen-based photochromic compounds, especially the parent

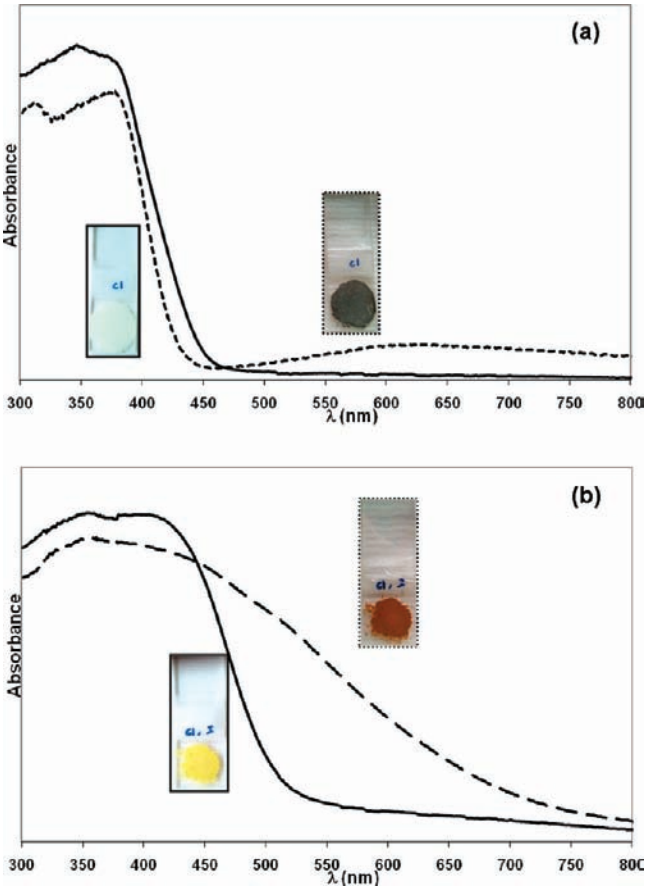

Figure 6. UV−vis spectra in the 200−800 nm range and photographs of samples of **2b** (a) and **4a** (b), before and after UV irradiation.

$(MV)[Bi_2Cl_8]$ compound, this feature is in favor of a photochromic mechanism involving the photoreduction of MV^{2+} to $MV^{\cdot+}$.[22] It is worth noting that the complete cancellation of color change occurs in the less iodide-doped compound ($(MV)[Bi_2Cl_{8-\varepsilon}I_\varepsilon]$), and this can be correlated to the 1D character of its inorganic network. In contrast, photochromism in the iodide-doped $n = 3$ compounds may be explained by the existence of all chloride clusters in structures. The alteration of photochromism in compounds containing iodide may be related, as in the case of polycyanopolycadmate clathrates of the second group (see above) or in a

(22) The presence of MV^+ is not confirmed from the EPR experiments that we carried out on irradiated **2b**. In fact, the weak signal that appears at very low temperature (Figure S5 in the SI) has a g value of 2.029, which is far from the g value of 2.003 assigned to the MV^+ radical.[10,13a,16b,18] While we checked both the absence of a peak in the EPR spectrum of a nonirradiated **2b** sample and that the $g = 2.029$ signal could be observed in different irradiated samples of **2b**, we were not able to assign the $g = 2.029$ peak to a known radical. Thus, the photochromic mechanism, which probably results from a photoinduced CT, remains questionable. In the case of the irradiated **4b** sample, we note the spread of the initial band in the visible region (Figure 6b), without a clear increase of specific bands assigned to $MV^{\bullet+}$, which also asks a question about the photochromic mechanism.

series of layered viologen phosphonates also containing either chloride, bromide, or iodide,[18] to the low ionization potential of iodide. Furthermore, no photochromism can be observed in recently synthesized iodo- (and bromo-) bismuthate salts of viologen, while as expected, a CT is observed.[23]

The most interesting feature of this series of compounds is that, on the one hand, they possess the same general structural layout as that described above and that, on the other hand, their photochromic behaviors are different. Despite the fact that we have already mentioned that the inorganic frameworks in all structures were built from (Bi_2Cl_8) subunits linked together by bridging chlorides (Cl_{bridg}), while nearly planar methylviologen dications were embedded between inorganic frameworks in the same behavior [the more distorted MV^{2+} are those located in the region of cleavage planes: dihedral angles between both cycles of 9.57° (**2b**), 12.15° (**3b**), and 18.90° (**4a** ($y \cong 0.65$)], we must emphasize that $BiCl_6$ octahedra are quite distorted in all structures with shorter Bi−Cl distances when Cl is a terminal chloride (Figures S2, S4, S7, and S10 in the SI). However, while the Bi−Cl_{bridg} distances are regular in (MV)[Bi_2Cl_8] (2.782 Å; Figure S11 in the SI) and in **1b** (2.873 and 2.855 Å; Figure S2 in the SI), they are quite different in **2b**, **3b**, and **4a** ($y \cong 0.65$), as a consequence of two types of octahedra (for **2b**, 2.998, 2.707, 2.720, and 2.970 Å; Figure S4 in the SI). Another main difference between **2b**, **3b**, or **4b** and **1b**, or **4a** is the presence of close $Cl_{terminal}\cdots Cl_{terminal}$ contacts in the former compounds. However, this structural feature seems not to be a key factor influencing the photochromic properties because crystals of **4a** and of **4b** undergo a similar behavior when irradiated by the UV lamp. By contrast, short $N^+\cdots Cl$ distances, or more generally short $N^+\cdots X$ interactions, exist in such photochromic materials.[10,11b,16b] In this way, all of our compounds are potentially photochromic because short $N^+\cdots Cl$ contacts, with Cl being almost perpendicular to the pyridinium ring at the nitrogen atom, as in (MV)[Bi_2Cl_8] [d = 3.441(1) Å], are observed: **1b**, N3···Cl9 3.329(4) Å, N1···Cl8 3.360(4) Å (Figure 2b); **2b**, N4···Cl10 3.366(4) Å, N2···Cl2 3.373(4) Å, N1···Cl8 3.381(4) Å (Figure 4); **3b**, N4···Cl10 3.347(4) Å, N2···Cl2 3.373(4) Å, N1···Cl8 3.383(4) Å (Figure S6 in the SI); **4a** ($y \cong 0.65$), N3···Cl3 3.356(4) Å, N2···Cl6 3.357(4) Å, N2···Cl2 3.393(4) Å (Figure S9 in the SI). Finally, let us note that side contacts, which are of the H···Cl type in the 2.60−2.80 Å range, are also present in all structures. Taking account these common structural features and the photochromic properties of the corresponding samples, we can conclude that the dimension of the oligomer size has a direct influence on photochromism. In a phosphonate viologen incorporating free Cl^-, photochromism was explained by the ability of the structure to stabilize $Cl^\bullet$, resulting from the CT.[18] It seems here that the small $n = 2$ cluster of $[Bi_4Cl_{18}]^{6-}$ is not able to exist as electron-deficient $[Bi_4Cl_{18}]^{5-}$ entities, or if it is, its lifetime is very short. In contrast, the $n = 3$ $[Bi_6Cl_{26}]^{8-}$ cluster and the infinite $[Bi_2Cl_8]^{2-}$ inorganic network ($n = \infty$) can probably exist as stable electron-deficient anions. This would explain the observed photochromic properties of the samples, which remain colored a few weeks in air at ambient conditions. Finally, a discoloration occurs, which probably results from an oxidation process by O_2, as described previously.[10,16b]

(23) Mercier, N. Unpublished results.

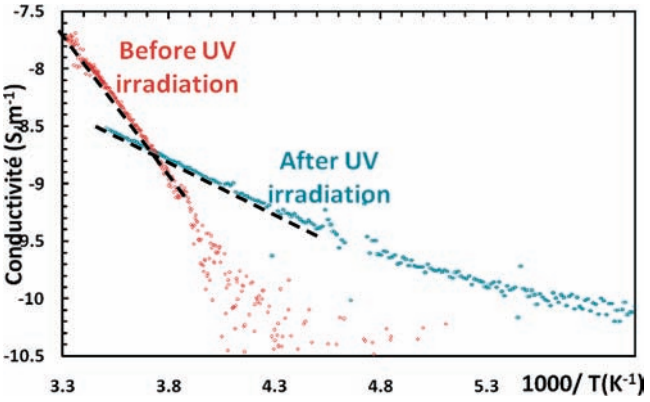

Figure 7. Conductivity of a single crystal of **2b**, before and after UV irradiation, as a function of the inverse of the temperature. Dotted lines represent the fits of the data by an Arrhenius law ($\ln \sigma \propto E_g/2k_BT$) shifted from the data for clarity.

Electrical Properties. The single-crystal conductivity of $(MV)_4[Bi_6Cl_{26}]$ (**2b**), before and after UV irradiation, as a function of the inverse of the temperature is shown in Figure 7 (see also the Experimental Section). The conductivity is extracted from the conductance by assuming that the current flows in the full thickness of the sample. In this respect, the measured values must be considered as minimum values. First, the room temperature conductivities of both crystals are quite low. These results are in good accordance with previous work on halobismuthates hybrids.[24] However, the low conductivity of irradiated **2b** also indicates that holes in the inorganic part and electrons on the methyviologen entities, which result from the photoinduced CT, are localized in the structure. Second, the band gap, which is calculated from the $\log(\sigma) = f(1000/T)$ curves, is smaller for the irradiated phase, 0.35 eV, compared to that for the crystal before irradiation (1 eV). It is interesting to note that the band gap of **2b** (before irradiation), extracted from the conductivity measurements, is much smaller than the optical gap extracted from UV−vis spectroscopy (Figure 6a), which is about 2.7 eV at ambient temperature. This optical gap is consistent with the yellow color of the sample and corresponds to the energy difference between the top of the valence band (main contribution of halide) and the bottom of the conduction band (main contribution of empty p orbitals of Bi^{III}), associated with the inorganic network.[9d,25] In contrast, the band gap extracted from electrical measurements may be explained by the difference between the LUMO of the organic part and the top of the valence band of the inorganic part. We recently carried out electrical measurements of $(MV)BiBr_5$, whose band gap was found to be 0.4 eV,[26] and it is worth noting that the higher value in **2b** (1 eV) is in good accordance with the expected lower energy of the top of the valence band in a chlorometalate compared to a bromometalate.[6a] In the hypothesis of an electron transfer from the inorganic cluster to the viologen dications upon irradiation, resulting in MV^+ radicals

(24) Gridunova, G. V.; Ziger, E. A.; Koshkin, V. M.; Struchkov, Y. T.; Shklover, V. E. *Zh. Neorg. Khim.* **1988**, *33*, 1718.
(25) Sourisseau, S.; Louvain, N.; Bi, W.; Mercier, N.; Rondeau, D.; Boucher, F.; Buzaré, J. Y.; Legein, C. *Chem. Mater.* **2007**, *19*, 600.
(26) Bi, W.; Leblanc, N.; Mercier, N.; Senzier, P.; Pasquier, C. *Chem. Mater.* **2009**, *21*, 4099.

(appearance of a broad band at 600 nm in the UV−vis spectrum:[12] see Figure 6a for **2b**) and electron-deficient inorganic entities, it would be expected that the HOMO of $MV^{\cdot+}$ decreases while the valence band associated with $[Bi_6Cl_{26}]$ increases. Also, this would explain the reduced band gap of irradiated **2b** (0.35 eV) calculated from the electrical measurements.

Conclusion

In summary, owing to the templating effect of the methylviologen dication (MV^{2+}), a series of chlorobismuthate hybrids $(MV)_{(2n+2)/2}[Bi_{2n}Cl_{8n+2}]$ ($n = 2$ and 3), whose structures can be related to the known structure of $(MV)[Bi_2Cl_8]$ ($n = \infty$) by the dimensional reduction concept, have been obtained. Two mixed halide hybrids, which can be considered as iodide-doped $n = 3$ clusters, with the formulas of $[Bi_6Cl_{25.6}I_{0.4}]^{8-}$ and $[Bi_6Cl_{24.6}I_{1.4}]^{8-}$, have been also characterized. All of these compounds result from the dehydration of as-synthesized corresponding hydrated hybrids. We showed that the dehydration process depends on the oligomer size and on the iodide rate. It can imply an impressive structural reorganization involving a 90° rotation of methylviologen dimers (in all of the $n = 3$ compounds) and a new Cl/I distribution inside the clusters. The photochromic properties of these materials have been investigated. It is found that the all-chloride compound $(MV)_4[Bi_6Cl_{26}]$ ($n = 3$) and $(MV)[Bi_2Cl_8]$ ($n = \infty$) undergo a color change from yellow to black, probably resulting from a photoinduced electron transfer from the inorganic networks to the organic entities. In contrast, the $(MV)_3[Bi_4Cl_{18}]$ hybrid does not exhibit photochromism, and this can be related to the inability of the $[Bi_4Cl_{18}]^{6-}$ oligomers to exist as electron-deficient entities. The main effect of the substitution of chlorides by iodides is an alteration of photochromism (color change from yellow to brown, instead of black in the case of all-chloride compounds) or even a complete cancellation of it for the iodide-doped $(MV)[Bi_2Cl_{8-\varepsilon}I_\varepsilon]$ hybrid. These behaviors may be explained by the low ionization potential of iodide, on the one hand, and by the 1D character of the inorganic network in $(MV)[Bi_2Cl_8]$, on the other hand. The single-crystal conductivity of $(MV)_4[Bi_6Cl_{26}]$, before and after UV irradiation, which has been carried out in the 180−300 K range, first indicates that room temperature conductivities of both crystals are quite low, showing, in particular, the localization of charges in the irradiated crystal. Interestingly, the band gap deduced from the electrical measurements is lower for the irradiated crystal, 0.35 eV compared to 1.0 eV for the crystal before irradiation. This feature, which could be correlated to organic radicals in the irradiated samples, as well as the photochromic mechanism, should be clarified in the future.

Acknowledgment. We thank the Pays de la Loire region for a postdoc fellowship to W.B. and for financial support through the MolTech program. Alain Mari from the LCC laboratory of Toulouse (France) is acknowledged for electron paramagnetic resonance (EPR) measurements.

Supporting Information Available: Crystallographic data in CIF format, single-crystal results, PXRD patterns, and thermal analysis (TGA and DSC) for **1a**−**4a**, UV−vis spectra of **3b** (after and before irradiation), and crystal structures of $(MV)_4[Bi_6Cl_{24.6}I_{1.4}](H_2O)_y$ (**4a**, $y \cong 0.65$) and $(MV)[Bi_2Cl_{8-\varepsilon}I_\varepsilon]$. This material is available free of charge via the Internet at http://pubs.acs.org.